ELSEVIER

International Journal of Inorganic Materials 3 (2001) 309–321

International Journal of Inorganic Materials

Preparation of ternary Bi–La and Bi–Pr oxides from polyaminocarboxylate complexes☆

Hilda Wullens, Daniel Leroy, Michel Devillers*

Université Catholique de Louvain, Unité de Chimie des Matériaux Inorganiques et Organiques, place Louis Pasteur, 1, B-1348 Louvain-la-Neuve, Belgium

Received 1 November 2000; accepted 23 March 2001

Abstract

Ternary bismuth–lanthanum and bismuth–praseodymium oxides are prepared by thermal decomposition of precursor complexes derived from solutions containing polyaminocarboxylate ligands: H_4edta, H_5dtpa, H_4egta and H_6ttha. The thermal decomposition of these solid precursors is investigated by TGA. The resulting Bi–La and Bi–Pr oxides are characterized by XRD, XPS analysis and S_{BET} measurements. XRD reveals the formation of $Bi_{2-x}Ln_xO_3$ solid solutions based on the fluorite-like δ-Bi_2O_3 structure when Bi:Ln=0.5 and Bi:Ln=1, while a rhombohedral phase appears when Bi:Ln=2. Surface contamination by hydroxyl and carbonate species increases with the Ln content. Specific surface areas as high as 30 m^2/g are obtained for the Ln-rich compositions. These results are compared with those obtained by the ceramic and citrate methods.

Keywords: Oxides; Chemical synthesis; X-ray diffraction; Photoelectron spectroscopy; Thermogravimetric analysis

1. Introduction

Great interest is devoted today to bismuth-based oxides because of the wide variety of materials where Bi is found either as an essential component or as an additive. For example, bismuth molybdates (Bi–Mo–O) are well-known to be effective industrial catalysts for the selective oxidation and for the ammoxidation of propene into acrolein and acrylonitrile [1]. Various Bi_2O_3-based systems have also been studied as catalysts for the oxidative coupling of methane to C_2-hydrocarbons [2]. In recent years, the newly discovered ferroelectric material $SrBi_2Ta_2O_9$ has been attracting profound interest as an alternative to lead zirconate titanate for non-volatile ferroelectric memories [3]. The cubic fluorite phase of bismuth oxide (δ-Bi_2O_3) is the best oxide ion conductor known so far, but its stability range is restricted to temperatures between 730 and 825°C. The stabilization of this phase at room temperature by partial substitution of numerous cations (namely lanthanides) for Bi^{3+} has attracted extensive attention [4–8]. Investigations in the past years in other Bi–M–O systems have led to the discovery of a new family of solid electrolyte named BIMEVOX (Bi–V–O and Bi–(V,M)–O) with very high oxide ion conductivity [9]. Since high-T_C superconductivity was first discovered in the Bi–Sr–Ca–Cu–O system by Maeda et al. [10], there have been numerous studies regarding the preparation and the structure of compounds belonging to this system. Finally, bismuth vanadium compounds ($BiVO_4$ and Bi–V–Mo–O) could play an important role in the world of pigments as potential substitutes for the toxic yellow lead chromate [11]. Because of its low water solubility and rapid elimination, bismuth is indeed considered to be the least toxic heavy metal used for industrial purpose nowadays [12].

The most commonly used method for preparing mixed oxides is the so-called ceramic route involving the component oxides or carbonates. Since the diffusion of the reactants is very slow in the solid state, the reaction requires a long heating time with intermediate grindings to achieve good homogeneity. The result is that the materials prepared by this way usually present poor properties such as lack of homogeneity and low surface area [13]. Consequently, there has been much interest in developing new strategies for materials synthesis that impart superior properties, particularly those involving soft chemical

☆Paper presented at the Second International Conference on Inorganic Materials, Santa Barbara, USA, 13–16 September, 2000.

*Corresponding author. Tel.: +32-10-472-827; fax: +32-10-472-330.
E-mail address: devillers@chim.ucl.ac.be (M. Devillers).

1466-6049/01/$ – see front matter
PII: S1466-6049(01)00036-8

routes [14]. Among them, a wide range of methods are known as the precursor methods. These procedures involving low temperature decomposition of suitable precursors have proven to be an advantageous alternative way to obtain complex materials (mixed oxides, solid solutions, sulphides, alloys . . .). In these methods, a better mixing of the cations is achieved and consequently, much shorter diffusion pathways are created. As far as oxide materials are concerned, controlled pyrolysis of amorphous citrate [15,16] or oxalate-type [17] precursors has frequently been used successfully to synthesize highly dispersed mixed oxides and solid solutions. Numerous applications can be found in the literature in the fields of high-T_C superconductors [18–21] and perovskites [22,23].

The present approach is a preparation method of multicomponent oxides containing bismuth and lanthanides based on the use of polyaminocarboxylate ligands (PAC): H_4edta (ethylenediaminetetraacetic acid), H_5dtpa (diethylenetriaminepentaacetic acid), H_4egta (ethyleneglycolbis(2-aminoethyl)tetraacetic acid) and H_6ttha (triethylenetetraaminehexaacetic acid).

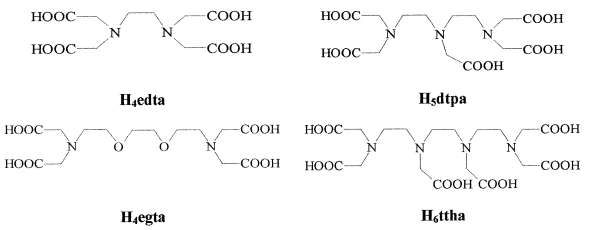

The choice of this particular class of ligands arises from several considerations

1. this class of ligands is well known to form soluble, very stable complexes with a wide range of metals
2. the obtained precursors contain no other element than C, H, N or O, avoiding thereby any contamination of the final material by S, P, halogens or alkali metals for example
3. the thermal decomposition of the complexes is complete at moderate temperatures, which are sufficiently low to limit the sintering effects
4. in addition, it can be shown that the residual carbon contamination of the oxide surface left by the organic part of the precursor is negligible.

Metal–PAC complexes have already been used to synthesize superconducting oxides. Y–Ba–Cu–O [24–26] and Bi–Pb–Sr–Ca–Cu–O [27] compounds have been prepared by various chelating methods using different ligands (H_3nta, H_4edta, H_3hedta (*N*-(2-hydroxyethyl)ethylenediaminetriacetic acid) and H_5dtpa), sometimes in the presence of coreagents like ethylenediamine to induce polymerization [28]. Similarly, La–Sr–Co–O or La–Sr–Mn–O perovskites have been prepared by the thermal decomposition of precursor complexes derived from nitrate solutions using edta [29–31]. Additional examples involving the use of edta-type precursors concern the preparation of $SrTiO_3$ [32], $BaTi_4O_9$ [33], lead magnesium niobate [34] and Bi-doped lanthanide iron garnets [35] as films or powders.

In the present case, the solid precursor is formed by the isomorphous complexes of component metals in the adequate ratio. This means that each metal is engaged with the same ligand to ensure a better homogeneity of the precursor. The precursor powder is then converted to the mixed oxide by thermal degradation under air. Within this context, the H_6ttha ligand establishes itself as an interesting candidate, because of its ability to form dinuclear molecular complexes. Oxides containing two different cations are synthesized more easily from a single molecular precursor exhibiting the required stoichiometry than from a mixture of precursors. This approach has already been described in the literature for the obtention of nickel ferrite [36] and lithium [37] or calcium [38] antimonates using edta-type precursors, or to synthesize Gd cuprate from a dtpa complex [39]. We have tested this procedure for the preparation of Bi–La and Bi–Pr mixed oxides. For comparative purposes, we also synthesised equivalent oxides by the citrate gel process, or by the ceramic route involving the component oxides (Bi–La) or carbonates (Bi–Pr). In this paper, we report the preparation of Bi–La and Bi–Pr PAC precursors and heterodinuclear Bi–La and Bi–Pr complexes with ttha ligand, the study of the thermal degradation of these complexes in air, the preparation of mixed oxides from these precursors, the preparation of the same oxides by the citrate route and the bulk and surface characterization of the mixed oxides obtained by X-ray diffractometry, X-ray photoelectron spectroscopy and surface area measurements (BET). Some preliminary results were already published elsewhere [40].

2. Experimental

2.1. Materials

Bismuth(III) oxide (α-Bi_2O_3, Alfa), bismuth(III) oxocarbonate ($(BiO)_2CO_3$, Fluka), bismuth(III) nitrate ($Bi(NO_3)_5 \cdot 5H_2O$, Fluka), lanthanum(III) oxide (La_2O_3, Aldrich), lanthanum(III) nitrate ($La(NO_3)_3 \cdot 6H_2O$, Aldrich), praseodymium(III, IV) oxide (Pr_6O_{11}, Acros), praseodymium(III) nitrate ($Pr(NO_3)_3 \cdot 6H_2O$, Aldrich) and praseodymium(III) carbonate ($Pr_2(CO_3)_3 \cdot xH_2O$, Alfa), all of p.a. purity were used as starting materials. The starting La_2O_3 was kept under an argon atmosphere since lanthanide oxides are very hygroscopic. H_5dtpa and H_4egta were purchased from Fluka, H_6ttha from Aldrich and H_4edta from Merck.

2.2. Preparation of mixed oxides by the ceramic method

Attempts to synthesise the Bi–Ln oxides according to the ceramic method were made using either the component

oxides (Bi–La/Pr systems) or carbonates (Bi–Pr system). These starting materials were ground in an agate mortar and calcined in air under different experimental conditions between 600 and 800°C.

2.3. Preparation of mixed oxides by the chelate method with H_4edta, H_5dtpa or H_4egta

Fig. 1 describes the preparation process of Bi–Ln–O mixed oxides (Ln=La or Pr) by the chelate method. The Bi and Ln complexes with H_4edta, H_5dtpa and H_4egta were obtained by dissolution of $(BiO)_2CO_3$ or La_2O_3 or $Pr_2(CO_3)_3$ in adequate proportions (molar ratio Bi:Ln= 0.5, 1 and 2) in aqueous solutions of the corresponding ligand (about 100 ml of water per gram of ligand). The molar ratio of the metal to the ligand was always 1:1. Only in the case of H_4edta, it was necessary to add NH_3 to raise the pH in order to achieve the formation of the La–edta complex. The colorless solutions were filtered off to remove the excess of metal reagent and then mixed with each other. The final solution was evaporated in a rotavapor and the resulting powder dried under vacuum at 40°C. This precursor powder was finally calcined under air flow in a tubular furnace at various temperatures for at least 2 h.

2.3. Preparation of mixed oxides by the chelate method with H_6ttha

The BiLn(ttha) compound was obtained by a different way. $(BiO)_2CO_3$ was added to a boiling aqueous solution of the ligand H_6ttha. The resulting suspension was stirred and heated until the bismuth reagent was completely dissolved. The solution containing the soluble $Bi(H_3ttha)$ complex was then filtered off to remove any excess of bismuth oxocarbonate. After addition of La_2O_3 or $Pr_2(CO_3)_3$, the suspension was stirred and heated at reflux for 24 h. The reagents were engaged in such a way that the Bi–Ln–ttha molar ratio was 1:1:1. The precipitate was then filtered off, washed with distilled water and dried in an oven at 40°C under vacuum. This precursor powder was finally calcined in a tubular furnace under an air flow at various temperatures for at least 2 h.

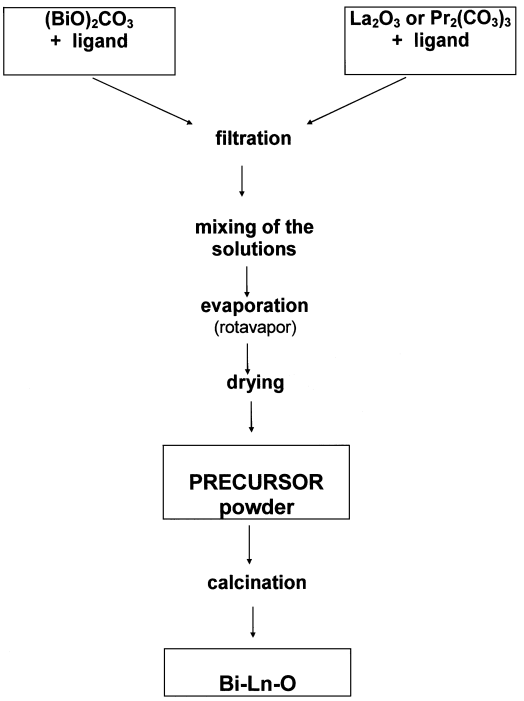

Fig. 1. Process flowsheet for sample preparation according to the chelate method.

2.4. Preparation of mixed oxides by the citrate method

Nitrate salts of bismuth ($Bi(NO_3)_3\cdot 5H_2O$), lanthanum ($La(NO_3)_3\cdot 6H_2O$) and praseodymium ($Pr(NO_3)_3\cdot 6H_2O$) were used as starting materials. The required amounts of bismuth nitrate and lanthanide (La or Pr) nitrates were dissolved separately in diluted nitric acid and distilled water, respectively. The individual nitrate solutions were mixed with citric acid engaged with 50% excess with respect to the metal. After mixing, the solution was evaporated on a rotavapor until a very viscous liquid was obtained. This gel was then heated in a vacuum oven at 80°C for 20 h. The amorphous solid foam obtained was calcined, after grinding, at 300°C in air for a further 20 h. After this precalcination step, the solid, after a subsequent grinding, was calcined in air at the final temperature for 20 h.

2.5. Sample characterization

The complexes and the precursor powders were characterized by IR spectroscopy, thermogravimetric analysis and C–H–N analysis. The Bi–La and Bi–Pr oxides were characterized by IR spectroscopy, XRD, XPS and measurement of their specific surface areas using the BET method. Infrared spectra were registered in the form of KBr pellets on a Bio-Rad FTS-135 Fourier transform spectrometer operating in the range 400–4000 cm^{-1}. Thermogravimetric analysis (TGA) was performed in air with a Mettler Toledo TGA/SDTA 851^e or a Setaram TGC85 analyser at a heating rate of 10°C min^{-1}. Powder X-ray diffraction spectra (XRD) were measured on a Siemens D-5000 diffractometer using the CuKα radiation (λ=1.5418 Å) and interpreted by reference to the JCPDS file. X-ray thermodiffractometry studies were carried out using a Siemens D-5000 X-ray diffractometer equipped with a Siemens HTK10 high temperature device (heating platinum plate). Diffractograms were registered at intervals of 100°C between 300 and 900°C and started after an isothermal step of 30 min. X-ray photoelectron spectra (XPS) were registered on a SSI-X-probe (SSX-100/206) spectrometer from Fisons, using a monochromatized AlKα radiation (E=1486.6 eV), under conditions of charge compensation (flood gun fixed at 10 eV). The analyses were based on the following peaks: C1s, O1s, Bi4f, $La3d_{5/2}$. The binding energy scale was calibrated with

respect to the C1s photopeak of hydrocarbon contamination fixed at 284.8 eV. The intensity ratio $I(Bi4f_{5/2})/I(Bi4f_{7/2})$ was fixed at 0.75.

The BET specific surface areas of the oxides were measured with a Micromeritics ASAP 2000 analyser, using krypton or nitrogen gas at 77 K.

3. Results and discussion

3.1. Starting complexes

Before being involved in the preparation of ternary oxides, the PAC complexes of Bi(III), La(III) and Pr(III) were isolated and characterized separately. The following complexes were isolated (with Ln = La or Pr): Bi(Hedta), (NH_4)Ln(edta), $(C(NH_2)_3)_2$Bi(dtpa), Ln(H_2dtpa), Bi(H_3ttha), La(H_3ttha), $(C(NH_2)_3)_2$Bi(Httha), $(C(NH_2)_2(NHNH_2))_2$Pr(Httha), $(C(NH_2)_3)_2$Ln(Httha), Bi_2(ttha), Ln_2(ttha), BiLn(ttha), Bi(Hegta), $Ln_4(egta)_3$. Their isolation and characterization are described elsewhere [41]. For some of these compounds, the crystal structure has been solved; this is the case for the following complexes: Bi(H_3ttha) [42], $(C(NH_2)_3)_2$Bi(Httha) [43], $(C(NH_2)_3)_2$Pr(Httha) and $(C(NH_2)_2(NHNH_2))_2$Pr(Httha) [41]. The crystal structures of Bi(Hedta), $(C(NH_2)_3)_2$Bi(dtpa) [44] and $(C(NH_2)_3)_2$La(Httha) [45] have been described by other authors.

3.2. Precursor synthesis

The mixed precursors based on edta, dtpa and egta ligands are actually a mixture of mononuclear complexes with the same type of ligand. For instance, a precursor with the overall stoichiometry $Bi_{1/3}La_{2/3}$(H_2dtpa) is, in fact, a mixture of one equivalent Bi(H_2dtpa) with two equivalents of La(H_2dtpa). For convenience, such a compound will be noted as $[Bi(dtpa)]_{1/3}[La(dtpa)]_{2/3}$ in the related tables. Each metal atom is chelated by one ligand molecule. The situation is completely different in the precursors based on ttha: BiLa(ttha) and BiPr(ttha). In this case, due to the fact that the decadentate ttha ligand is able to pick up two different metal atoms in the complex, the precursor molecule is a heterobinuclear complex where the two metal atoms are chelated by the same ligand molecule. It is therefore impossible to change the Bi:La molar ratio in the latter case, but this precursor presents the great advantage of ensuring a perfect mixing of the two metals at the atomic scale.

In the case of the edta ligand, the experimental procedure is slightly different from the general procedure: addition of NH_3 to a pH of 7 is necessary to complete complexation of the lanthanide by edta, and precursors containing ammonium as counterions, (NH_4)M(edta), are therefore observed. With egta and dtpa, the stability constants are sufficiently high to ensure La or Pr complexation without pH control. Stability constants of PAC complexes with Bi are so high that complexation can be achieved without any pH raising [46]. Complexes of Bi, La and Pr with edta, dtpa and egta are characterized by an extensive water solubility, contrary to BiLn(ttha) (Ln = La or Pr) which is totally insoluble.

3.3. Thermal decomposition of the mixed oxide precursor

Whatever the nature of the ligand, or the Bi:Ln ratio, the thermal decomposition of the precursors always proceeds in three major steps: first, dehydration of the complex followed by the ligand pyrolysis to a carbonate stage and finally, removal of CO_2 leading to a crystalline mixed oxide. The nature of this mixed oxide is discussed in another section. All the precursors (with edta, dtpa and egta) behave in a similar way except BiLn(ttha) which will be discussed separately. The analogy between the thermal decomposition of the La and Pr precursors is remarkable and, consequently, they will be discussed together without any distinction between La and Pr. The main relevant data are presented in Tables 1 and 2 for Bi–La and Bi–Pr systems, respectively. The theoretical water contents listed in column 9 of these tables refer to the stoichiometry given in column 1, as determined from the experimental value of the first weight loss in the TG curves (column 10). The theoretical total weight losses listed in column 11 are calculated assuming that the residual oxide corresponds to the stoichiometric formula $Bi_{2-x}Ln_xO_3$. In both cases, calculated and experimental values agree pretty well with each other.

Figs. 2 and 3 present the thermogravimetric curves of the Bi–La precursors with edta and dtpa, respectively. The egta precursors display the same type of decomposition. The dehydration step spreads over a wide temperature range: from about 60 to 220°C. The ligand pyrolysis begins near 250°C and ends around 400°C. It can be divided in three or four substeps, following the inflexions of the curve. When the Ln:Bi molar ratio increases, the curve displays a more ‘staircase’ look and the number of subdivisions in this second step increases. The first mass loss in this second step begins with a slow process (column 1), followed by a faster one (columns 2a and 2b). The third major stage (column 3) in the precursor thermal decomposition lies around 450–550°C and must be related to inorganic residue evolution because it is quite independent of the ligand nature. It consists of the decomposition of the carbonate species formed at the end of the ligand pyrolysis into an oxocarbonate $(MO)_2CO_3$ intermediate. Finally, this mixed oxocarbonate decomposes to the mixed oxide in a very soft process (column 4). Sometimes, in Bi-richer precursors based on dtpa, the oxocarbonate stage is not visible. The final decomposition temperature increases with the Ln–Bi molar ratio, which reflects the great stability of the lanthanide carbonates.

Table 1
TGA data of the Bi–La precursors

Precursor[a]	Decomposition steps (°C)						T_f	Weight loss (%)			
	Dehydr.	1	2a	2b	3	4		Dehydration		Total	
								Calc.[b]	Exp.[c]	Calc.[d]	Exp.[e]
$[Bi(edta)]_{2/3}[La(edta)]_{1/3}\cdot 2H_2O$	80–115	255–285	285–395		450–470	470–495	495	6.8	6.3	60.3	67.8
$[Bi(edta)]_{1/2}[La(edta)]_{1/2}\cdot 2H_2O$	60–170	265–290	290–380	380–390	450–470	470–540	540	7.0	6.6	61.7	61.6
$[Bi(edta)]_{1/3}[La(edta)]_{2/3}\cdot 2H_2O$	60–120	250–290	290–370	370–395	450–480	480–570	570	7.1	7.5	63.1	62.8
$[Bi(dtpa)]_{2/3}[La(dtpa)]_{1/3}\cdot 2.5H_2O$	65–175	235–240	285–385		430–515	–	515	7.2	6.6	66.2	72.0
$[Bi(dtpa)]_{1/2}[La(dtpa)]_{1/2}\cdot 1.5H_2O$	70–170	225–250	290–370	370–380	445–465	465–530	530	4.6	4.9	66.5	67.7
$[Bi(dtpa)]_{1/3}[La(dtpa)]_{2/3}\cdot 1.5H_2O$	85–180	240–250	290–365	365–380	460–485	485–565	565	4.7	4.5	67.9	68.2
$[Bi(egta)]_{2/3}[La(egta)]_{1/3}\cdot 1.5H_2O$	80–150	220–260	260–380		430–460	460–505	505	4.6	4.2	64.5	65.0
$[Bi(egta)]_{1/2}[La(egta)]_{1/2}\cdot 1H_2O$	50–150	220–270	270–385		450–465	465–550	550	3.2	3.5	65.2	65.4
$[Bi(egta)]_{1/3}[La(egta)]_{2/3}\cdot 1.5H_2O$	60–160	220–275	275–360	360–395	465–500	500–600	600	4.8	4.4	67.1	68.8
$BiLa(ttha)\cdot 6.5H_2O$	100–125	–		295–325		325–500	500	12.3	12.4	58.5	58.5

[a] Proton and ammonium counter-ions have been omitted in the formula.
[b] Calculated dehydration weight loss $= n\ H_2O\cdot M_{H_2O}/M_{precursor}$.
[c] Experimental dehydration weight loss.
[d] Calculated total weight loss $= (M_{precursor} - M_{oxide})/M_{precursor}$ assuming the oxide stoichiometry $Bi_{2-x}Ln_xO_3$.
[e] Experimental total weight loss.

The heteronuclear BiLn(ttha) compound (Ln = La or Pr) decomposes itself in a much simpler way. After dehydration, the ligand pyrolysis occurs in a single step leading directly to the mixed oxocarbonate stage (BiO)(LnO)(CO_3) (for Pr: TG loss: 51.7%, calc.: 52.40%; for La: TG loss: 53.9%, calc.: 53.86%). Then, the oxocarbonate releases slowly one CO_2 molecule to produce the mixed oxide $BiLnO_3$. It has not been possible to confirm the presence of the oxocarbonate by XRD because of the amorphous nature of this intermediate.

3.4. XRD characterization of the mixed oxides

The nature of the final oxides obtained after calcination in air has been determined by powder XRD. Tables 3–5 summarize the results observed with the ceramic method, the polyaminocarboxylate and the citrate precursors, respectively. Here again, great analogy is observed between La and Pr-based compounds but some differences in the nature of the final phase are, however, sometimes observed.

3.4.1. Ceramic method

In the case of the Bi–La system, attempts were made to use the ceramic method to prepare certain ternary Bi–La–O phases whose compositions correspond to already described systems: $Bi_{1.92}La_{0.08}O_3$ (JCPDS No 41-0273, tetragonal), $Bi_{1.88}La_{0.12}O_3$ (41-0292, cubic), $Bi_{0.775}La_{0.225}O_{1.5}$ (48-0346, rhombohedral) and the cubic solid solution δ-$Bi_{2-x}La_xO_3$ (based on the δ-Bi_2O_3 phase, 16-0654). Some other compositions were also considered. In the Bi-rich samples (Bi/La = 24, 15.7, 4.7 and 3.0), there is no trace of La oxide except in very low amounts in the last of these compositions. On the other hand, α-Bi_2O_3 appears only after heating at 800°C for 4 h for the Bi/La ratio of 15.7. For all four compositions mentioned above,

Table 2
TGA data of the Bi–Pr precursors

Precursor[a]	Decomposition steps (°C)						T_f	Weight loss (%)			
	Dehydr.	1	2a	2b	3	4		Dehydration		Total	
								Calc.[b]	Exp.[c]	Calc.[d]	Exp.[e]
$[Bi(dtpa)]_{2/3}[Pr(dtpa)]_{1/3}\cdot 1.5H_2O$	85–230	255–265	290–410		475–565	–	565	4.5	4.6	72.9	66.8
$[Bi(dtpa)]_{1/2}[Pr(dtpa)]_{1/2}\cdot 1.5H_2O$	90–220	225–295	295–390		450–510	–	510	4.6	4.3	66.4	64.9
$[Bi(dtpa)]_{1/3}[Pr(dtpa)]_{2/3}\cdot 2.5H_2O$	50–220	235–275	275–375	375–385	460–545	545–700	700	7.5	7.8	68.6	70.0
$[Bi(egta)]_{2/3}[Pr(egta)]_{1/3}.2H_2O$	70–210	240–285	285–290	290–415	475–540	540–620	620	6.0	5.6	65.9	63.9
$[Bi(egta)]_{1/2}[Pr(egta)]_{1/2}\cdot 2H_2O$	65–210	240–285	285–295	295–425	500–565	565–720	720	6.1	6.1	66.2	68.0
$[Bi(egta)]_{1/3}[Pr(egta)]_{2/3}\cdot 2.5H_2O$	65–160	250–295	295–300	300–425	485–555	555–740	740	7.7	7.3	68.0	68.3
$BiPr(ttha)\cdot 5H_2O$	140–170	–		315–390			390	9.7	9.5	57.1	55.9

[a] Proton and ammonium counter-ions have been omitted in the formula.
[b] Calculated dehydration weight loss $= nH_2O\cdot M_{H_2O}/M_{precursor}$.
[c] Experimental dehydration weight loss.
[d] Calculated total weight loss $= (M_{precursor} - M_{oxide})/M_{precursor}$ assuming the oxide stoichiometry $Bi_{2-x}Ln_xO_3$.
[e] Experimental total weight loss.

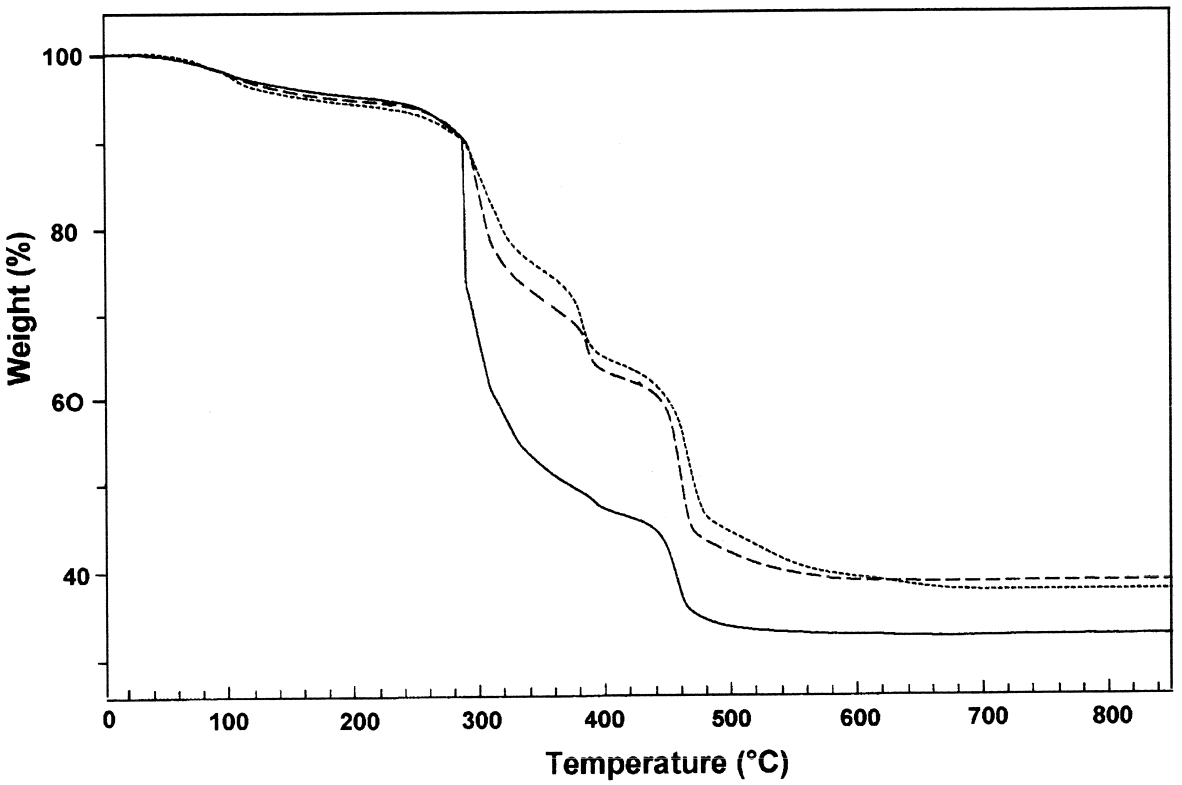

Fig. 2. TGA curves of $[Bi(edta)]_x[La(edta)]_{1-x}$ precursors [$x=0.33$ (···), 0.50 (- - -), 0.67(—)].

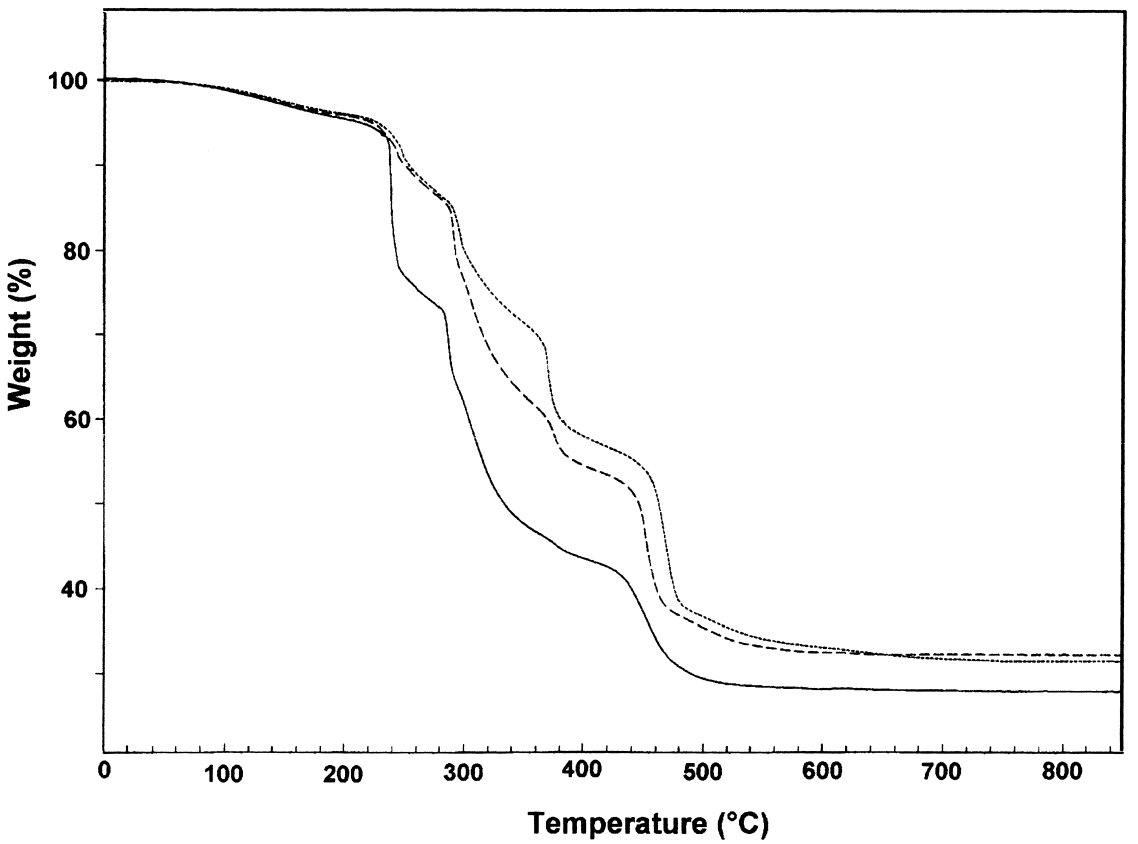

Fig. 3. TGA curves of $[Bi(dtpa)]_x[La(dtpa)]_{1-x}$ precursors [$x=0.33$ (···), 0.50 (- - -), 0.67(—)].

Table 3
XRD identification of the Bi–Ln–O samples obtained by the ceramic route

Starting mixture	Calcination conditions T (°C), t (h)	Bi/Ln	Phases detected[a]
$Bi_2O_3 + La_2O_3$	800, 96	24	$Bi_{1.88}La_{0.12}O_3$ (vs), $Bi_{0.775}La_{0.225}O_{1.5}$ (vw)
	800, 4	15.7	$Bi_{1.92}La_{0.08}O_3$ (vs), $Bi_{1.88}La_{0.12}O_3$ (vs), Bi_2O_3 (s), $Bi_{0.775}La_{0.225}O_{1.5}$ (vw)
	800, 96		$Bi_{1.88}La_{0.12}O_3$ (vs), $Bi_{0.775}La_{0.225}O_{1.5}$ (vw)
	800, 4	4.7	$Bi_{0.775}La_{0.225}O_{1.5}$ (vs), $Bi_{1.88}La_{0.12}O_3$ (s)
	800, 96		$Bi_{0.775}La_{0.225}O_{1.5}$ (vs), $Bi_{1.88}La_{0.12}O_3$ (vw)
	800, 4	3.0	$Bi_{0.775}La_{0.225}O_{1.5}$ (vs), $Bi_{1.88}La_{0.12}O_3$ (vw), La_2O_3 (vw)
	700, 4	1.0	$Bi_{0.775}La_{0.225}O_{1.5}$ (vs), La_2O_3 (s), Bi_2O_3 (vw)
	800, 4		$Bi_{0.775}La_{0.225}O_{1.5}$ (s), δ $Bi_{2-x}La_xO_3$ (s), La_2O_3 (m)
	800, 96		δ-$Bi_{2-x}La_xO_3$ (vs), $Bi_{0.775}La_{0.225}O_{1.5}$ (s), La_2O_3 (vw)
	800, 4	0.33	La_2O_3 (vs), $Bi_{0.775}La_{0.225}O_{1.5}$ (w)
$Bi_2O_3 + Pr_6O_{11}$	700, 48	2.0	$Bi_{0.775}Pr_{0.225}O_{1.5}$ (vs), Pr_6O_{11} (w), δ-$Bi_{2-x}Pr_xO_3$ (vw)
	800, 48		$Bi_{0.775}Pr_{0.225}O_{1.5}$ (vs), δ-$Bi_{2-x}Pr_xO_3$ (vw)
	700, 48	1.0	$Bi_{0.775}Pr_{0.225}O_{1.5}$ (vs), Pr_6O_{11} (s), δ-$Bi_{2-x}Pr_xO_3$ (vw)
	800, 48		$Bi_{0.775}Pr_{0.225}O_{1.5}$ (vs), Pr_6O_{11} (s), δ-$Bi_{2-x}Pr_xO_3$ (vw)
	700, 48	0.5	$Bi_{0.775}Pr_{0.225}O_{1.5}$ (vs), Pr_6O_{11} (s)
	800, 48		$Bi_{0.775}Pr_{0.225}O_{1.5}$ (vs), Pr_6O_{11} (s)
$Bi_2CO_5 + Pr_2(CO_3)_3$	700, 48	2.0	$Bi_{0.775}Pr_{0.225}O_{1.5}$
	700, 48	1.0	$Bi_{0.775}Pr_{0.225}O_{1.5}$ (vs), Pr_6O_{11} (s)
	700, 48	0.5	$Bi_{0.775}Pr_{0.225}O_{1.5}$ (vs), Pr_6O_{11} (s)

[a] Abbreviations: vs, very strong (>80%); s, strong (50/80%); m, medium (25/50%); w, weak (10/25%); vw, very weak (<10%).

the corresponding mixed oxide was never obtained in pure form and the XRD patterns indicate a mixture of the cubic $Bi_{1.88}La_{0.12}O_3$ and rhombohedral $Bi_{0.775}La_{0.225}O_{1.5}$ phases, the latter being the major one except for the two Bi-richest compositions under extreme calcination conditions (800°C, 24 h). For the equimolar composition (Bi/La=1), the rhombohedral $Bi_{0.775}La_{0.225}O_{1.5}$ phase appears systematically, together with La_2O_3 and the cubic solid solution which appears at 800°C. At 700°C/4 h, the rhombohedral phase is the only mixed phase generated and coexists with the two binary oxides. For the Ln-rich composition investigated (Bi/La=0.33), small amounts of the mixed rhombohedral phase appear with La_2O_3 as major component.

Three different compositions were considered in the case of the Bi/Pr system (Bi/Pr=2.0, 1.0 and 0.5). When starting from the corresponding binary oxides heated at 700 or 800°C, the rhombohedral $Bi_{0.775}Pr_{0.225}O_{1.5}$ phase is omnipresent whatever the overall composition and is accompanied by large amounts of Pr_6O_{11} for Bi/Pr=0.5, by smaller amounts of this oxide but also very small amounts of the cubic δ-$Bi_{2-x}Pr_xO_3$ solid solution for Bi/Pr=1.0. In the case Bi/Pr=2.0, the rhombohedral phase is still present but coexists essentially with the solid solution and also small amounts of Pr_6O_{11} at 700°C. When starting from carbonates, the rhombohedral phase is obtained in pure form when Bi/Pr=2.0, and is accompanied by Pr_6O_{11} for the two Bi-richer compositions. In these interpretations, the diffraction lines assigned to Pr_6O_{11} are always very slightly shifted towards larger diffraction angles, suggesting that small amounts of Bi could be incorporated in the lattice.

In conclusion, the rhombohedral $Bi_{0.775}Ln_{0.225}O_{1.5}$ phase is omnipresent in all these samples whatever the starting composition and the solid solution appears more easily when the Ln content increases, but never in pure form.

3.4.2. Chelate and citrate methods

Though the formation of α-Bi_2O_3, La_2O_3 and Pr_6O_{11} was systematically confirmed after calcination of pure Bi, La and Pr polyaminocarboxylate respectively, the constituent oxides (Bi_2O_3, La_2O_3, Pr_2O_3 and Pr_6O_{11}) have never been observed in the products obtained after calcination of the mixed precursors for the Bi/Ln molar ratios presently investigated. Only ternary Bi–Ln–O phases are detected in the samples prepared by the citrate or the chelate methods.

When Ln/Bi=2 (Ln=La or Pr), whatever the precursor nature (citrate or chelate), a solid solution based on δ-Bi_2O_3 is formed: δ-$Bi_{2-x}Ln_xO_3$. The high temperature δ phase of Bi_2O_3 crystallizes in a defect fluorite structure with 25% of the oxide ion sites unoccupied. This phase is well known because it is the best oxide ion conductor known so far [47] but is stable only between 730 and 825°C, the fusion temperature of bismuth sesquioxide [48,49]. Stabilization of this phase to room temperature by substitution of various cations for Bi has been the subject of many studies. A solid solution between δ-Bi_2O_3 and Pr_6O_{11} is not surprising since both of them have the same related defect fluorite structure [50]. Contrary to Pr, La_2O_3 does not present the fluorite structure but a solid solution between La_2O_3 and Bi_2O_3 is nevertheless observed for that composition. In the latter case, no shift is observed

Table 4
XRD identification of the thermal decomposition products of Bi – Ln (Ln=La, Pr) polyaminocarboxylate precursors[a,b]

Precursor[c]		Calcination conditions		
		600°C, 2 h	600°C, 20 h	800°C, 2 h
$[Bi(edta)]_{1/3}[Ln(edta)]_{2/3}$	La	δ-$Bi_{2-x}Ln_xO_3$	δ-$Bi_{2-x}Ln_xO_3$	δ-$Bi_{2-x}Ln_xO_3$
$[Bi(dtpa)]_{1/3}[Ln(dtpa)]_{2/3}$	Pr	δ-$Bi_{2-x}Ln_xO_3$	–	δ-$Bi_{2-x}Ln_xO_3$
	La	δ-$Bi_{2-x}Ln_xO_3$	δ-$Bi_{2-x}Ln_xO_3$	δ-$Bi_{2-x}Ln_xO_3$
$[Bi(egta)]_{1/3}[Ln(egta)]_{2/3}$	Pr	δ-$Bi_{2-x}Ln_xO_3$	–	δ-$Bi_{2-x}Ln_xO_3$
	La	δ-$Bi_{2-x}Ln_xO_3$	δ-$Bi_{2-x}Ln_xO_3$	δ-$Bi_{2-x}Ln_xO_3$
$[Bi(edta)]_{1/2}[Ln(edta)]_{1/2}$	La		δ-$Bi_{2-x}Ln_xO_3$	δ-$Bi_{2-x}Ln_xO_3$ (R–$Bi_{2-x}Ln_xO_3$)
$[Bi(dtpa)]_{1/2}[Ln(dtpa)]_{1/2}$	Pr	δ-$Bi_{2-x}Ln_xO_3$ (R–$Bi_{2-x}Ln_xO_3$)	–	δ-$Bi_{2-x}Ln_xO_3$ (R–$Bi_{2-x}Ln_xO_3$)
	La		δ-$Bi_{2-x}Ln_xO_3$ (R–$Bi_{2-x}Ln_xO_3$)	$Bi_8La_{10}O_{27}$ (R–$Bi_{2-x}Ln_xO_3$)
$[Bi(egta)]_{1/2}[Ln(egta)]_{1/2}$	Pr	δ-$Bi_{2-x}Ln_xO_3$ (R–$Bi_{2-x}Ln_xO_3$)	–	δ-$Bi_{2-x}Ln_xO_3$ (R–$Bi_{2-x}Ln_xO_3$)
	La		δ-$Bi_{2-x}Ln_xO_3$ (R–$Bi_{2-x}Ln_xO_3$)	$Bi_8La_{10}O_{27}$ (R–$Bi_{2-x}Ln_xO_3$)
BiLn(ttha)	Pr	δ–$Bi_{2-x}Ln_xO_3$	–	δ-$Bi_{2-x}Ln_xO_3$
	La	δ-$Bi_{2-x}Ln_xO_3$	δ-$Bi_{2-x}Ln_xO_3$	δ-$Bi_{2-x}Ln_xO_3$
$[Bi(edta)]_{2/3}[Ln(edta)]_{1/3}$	La		R–$Bi_{2-x}Ln_xO_3$	R–$Bi_{2-x}Ln_xO_3$
$[Bi(dtpa)]_{2/3}[Ln(dtpa)]_{1/3}$	Pr	R–$Bi_{2-x}Ln_xO_3$ (δ-$Bi_{2-x}Ln_xO_3$)	–	R–$Bi_{2-x}Ln_xO_3$
	La		R–$Bi_{2-x}Ln_xO_3$ (δ-$Bi_{2-x}Ln_xO_3$)	R–$Bi_{2-x}Ln_xO_3$ (δ-$Bi_{2-x}Ln_xO_3$)
$[Bi(egta)]_{2/3}[Ln(egta)]_{1/3}$	Pr	R–$Bi_{2-x}Ln_xO_3$ (δ-$Bi_{2-x}Ln_xO_3$)	–	R–$Bi_{2-x}Ln_xO_3$
	La		R–$Bi_{2-x}Ln_xO_3$ (δ-$Bi_{2-x}Ln_xO_3$)	R–$Bi_{2-x}Ln_xO_3$ (δ-$Bi_{2-x}Ln_xO_3$)

[a] Phases between parentheses are very low abundant in the XRD pattern.
[b] R–$Bi_{2-x}Ln_xO_3$ refers to the rhombohedral phase $Bi_{0.775}Ln_{0.225}O_{1.5}$ corresponding to the JCPDS files No. 48-0346 for La and to No. 48-0347 for Pr.
[c] Proton and ammonium counter-ions have been omitted in the formula.

Table 5
XRD identification of the thermal decomposition products of Bi:Ln (Ln=La, Pr) citrate precursors

Ln/Bi		Calcination conditions[a]	
		600°C, 20 h	700°C, 20 h
2	Pr	δ-$Bi_{2-x}Ln_xO_3$	–
	La	δ-$Bi_{2-x}Ln_xO_3$	δ-$Bi_{2-x}Ln_xO_3$
1	Pr	δ-$Bi_{2-x}Ln_xO_3$ (R–$Bi_{2-x}Ln_xO_3$)	–
	La	δ-$Bi_{2-x}Ln_xO_3$ (R–$Bi_{2-x}Ln_xO_3$)	δ-$Bi_{2-x}Ln_xO_3$ (R–$Bi_{2-x}Ln_xO_3$)
0.5	Pr	R–$Bi_{2-x}Ln_xO_3$ (δ-$Bi_{2-x}Ln_xO_3$)	–
	La	R-$Bi_{2-x}Ln_xO_3$ (δ-$Bi_{2-x}Ln_xO_3$)	R–$Bi_{2-x}Ln_xO_3$ (δ-$Bi_{2-x}Ln_xO_3$)

[a] Phases between parentheses are very low abundant in the XRD pattern; R–$Bi_{2-x}Ln_xO_3$ refers to the rhombohedral phase $Bi_{0.775}Ln_{0.225}O_{1.5}$ corresponding to the JCPDS files No. 48-0346 for La and to No. 48-0347 for Pr.

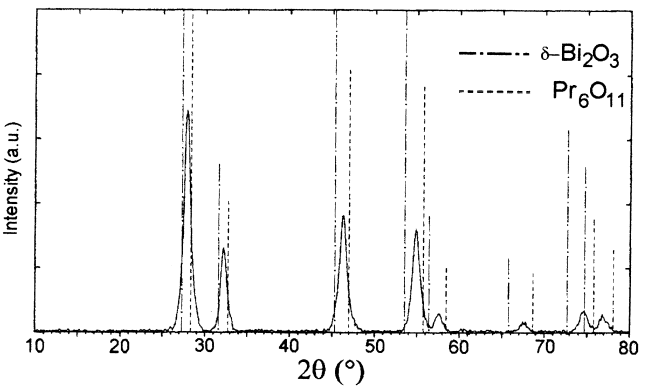

Fig. 4. XRD pattern of the Bi–Pr–O oxide obtained by calcination of the BiPr(ttha) precursor at 500°C for 8 h. The position of the lines for δ-Bi_2O_3 (JCPDS-No. 16-0654) and Pr_6O_{11} (JCPDS-No. 6-0329) are indicated by broken lines.

from the position of δ-Bi_2O_3 peaks, as expected on the basis of the ionic radii of Bi and La cations which are almost identical (in eightfold coordination: $r^{3+}_{Bi}=131$ pm; $r^{3+}_{La}=130$ pm) [51]. As illustrated in Fig. 4 for Bi/Pr=1, the difference between r^{3+}_{Bi} and r^{3+}_{Pr} ($r^{3+}_{Pr}=126.6$ pm) is naturally reflected in a shift in the diffraction lines, the partial substitution of the smaller Pr cation for Bi leading to a lattice contraction.

When Bi and La are engaged in equimolar proportions, a new ternary rhombohedral Bi–La–O phase corresponding to $Bi_{0.775}La_{0.225}O_{1.5}$ appears in small quantities. This is the case for both the citrate and the chelate methods but not when the heterometallic BiLa(ttha) precursor is used. Calcination of BiLa(ttha) up to 850°C leads to a pure solid solution δ-$Bi_{2-x}La_xO_3$. A similar behaviour is observed in the Bi–Pr–O system with Bi/Pr=1: the pure solid solution appears after calcination of BiPr(ttha) at 600 or 800°C, while the use of dtpa and egta precursors generates minor amounts of the rhombohedral phase corresponding to $Bi_{0.775}Pr_{0.225}O_{1.5}$. The latter phase is somewhat more abundant in the samples obtained by the citrate route.

When the molar ratio Ln:Bi equals 0.5, the diffractograms reveal the presence of the rhombohedral phase as the major phase and the δ-solid solution as a minor component, for the two lanthanides and whatever the precursor nature.

X-ray diffractometry has also been used to observe the high temperature modifications during a heating run between 300 and 900°C. Fig. 5 presents a series of XRD patterns of the BiLa(ttha) precursor taken at intervals of 100°C, showing the formation of the δ-solid solution and the appearance of small peaks at 900°C, that can be attributed to the rhombohedral phase. For samples calcined at 500°C for 2 h, oxocarbonate species can be sometimes detected in the diffractograms.

3.5. XPS characterization of Bi–La–O oxides

As pyrolysis of the organic skeleton of the ligand could be at the origin of a high carbon contamination, XPS analysis was performed in order to control the surface chemical composition.

Beside the two usual components of the C1s peak at 284.8 and 286.3 eV assigned to C–(C,H) and C–O, respectively, a third peak lying in the range 288.9–289.3 eV is present in the C1s spectra. This peak may be explained by the presence of carbonate species at the surface. It is well known that lanthanides show a great affinity for carbonate and hydroxyl species. Earlier studies [52,53] have shown that upon exposure to atmospheric H_2O and CO_2, lanthana transforms into a partly carbonated hydroxide. The final lanthanum oxide stabilized in air consists actually of a nucleus of crystalline $La(OH)_3$ surrounded by hydroxycarbonate phase.

For all the samples, the O 1s signals could be fitted with two peaks: one with a maximum around $E_b=529.0$ eV (O_I) and a second around 531.3 eV (O_{II}). In accordance with several earlier studies [54,55], the oxygen peak at the lower binding energy is attributed to lattice oxygen. The binding energy associated with O_I (529.0–529.2 eV) for Bi–La–O mixed oxides lies between the corresponding values for pure Bi_2O_3 (529.5) and pure La_2O_3 (528.6 eV). We attribute the broad peak at higher binding energy to hydroxyl and carbonate groups chemisorbed on the oxide. This peak at the higher binding energy has been interpreted as adsorbed oxygen or hydroxyl groups by other authors

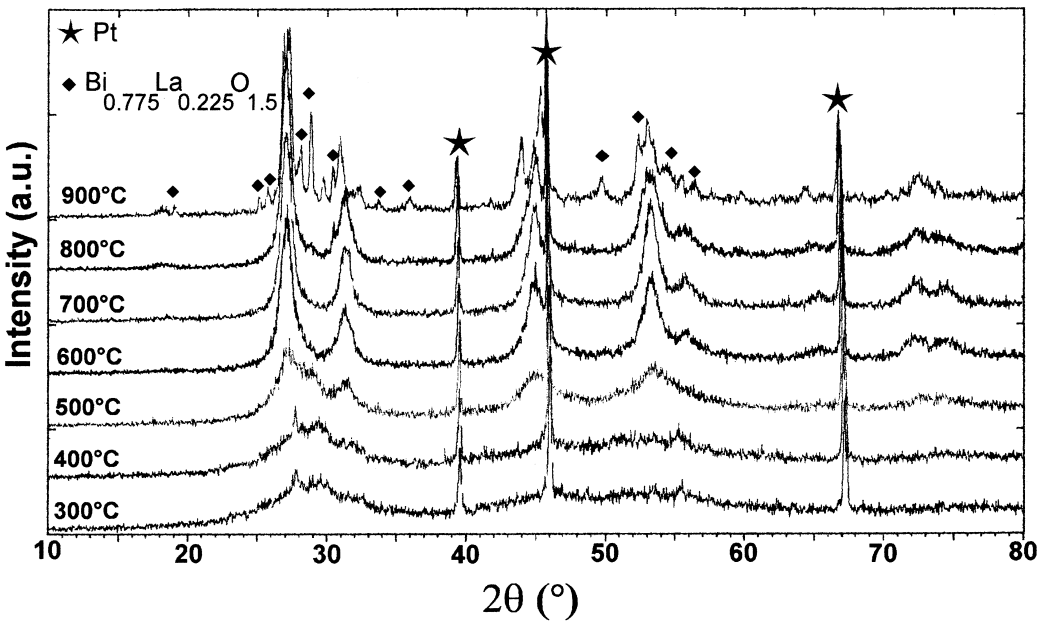

Fig. 5. X-ray thermodiffractograms of the BiLa(ttha) precursor calcined in situ between 300 and 900°C; ♦, R–$Bi_{0.775}La_{0.225}O_{1.5}$; ★, Pt support.

Table 6
XPS characterization of the Bi–La–O oxides obtained by the chelate method 600°C 20 h

Precursor[a]	C1s/ (Bi4f + La3d$_{5/2}$)	Bi4f/ La3d$_{5/2}$	O_{II}/O_I
[Bi(edta)]$_{1/3}$[La(edta)]$_{2/3}$	2.15	0.90	1.19
[Bi(dtpa)]$_{1/3}$[La(dtpa)]$_{2/3}$	2.35	0.85	1.20
[Bi(egta)]$_{1/3}$[La(egta)]$_{2/3}$	2.38	0.83	0.87
[Bi(edta)]$_{1/2}$[La(edta)]$_{1/2}$	1.56	1.70	0.65
[Bi(dtpa)]$_{1/2}$[La(dtpa)]$_{1/2}$	1.64	1.52	0.57
[Bi(egta)]$_{1/2}$[La(egta)]$_{1/2}$	1.80	1.72	0.57
BiLa(ttha)	1.65	1.74	0.67
[Bi(edta)]$_{2/3}$[La(edta)]$_{1/3}$	1.48	3.39	0.45
[Bi(dtpa)]$_{2/3}$[La(dtpa)]$_{1/3}$	1.51	3.04	0.61
[Bi(egta)]$_{2/3}$[La(egta)]$_{1/3}$	1.59	2.90	0.52

[a] Proton and ammonium counter-ions have been omitted in the formula.

[56] for Bi-based oxides partially substituted by Y, Zr, or Pr. However, the presence of a third component at 289 eV in our C 1s spectra led us to interpret the O_{II} component by the presence of both hydroxyl and carbonate groups. For comparative purposes, the O1s component in the corresponding Bi oxocarbonate ($Bi_2O_2CO_3$) appears at 530.4 eV.

No significant variations in Bi or La binding energies are observed between the samples prepared by the chelate or the citrate method and between the samples of different Bi:La molar ratios. The 4f spectra of Bi display one doublet which can be assigned to Bi(III). The binding energies values associated with the Bi $4f_{7/2}$ photopeak lie in the range 158.5–158.8 eV which correspond to the value typically observed in Bi oxides.

The La $3d_{5/2}$ photoemission peak is accompanied by a satellite appearing at some 4 eV towards higher binding energies from the main peak. The satellite is interpreted in terms of the excitation of an electron from the anion O2p valence band into the lanthanum 4f band [57]. However, the shape of the main peak at lower binding energy is broadened for the Bi–La–O mixed oxides. It was thus necessary to include additional components at higher binding energies to obtain a satisfactory fit of the experimental data. In the literature, the value for the La $3d_{5/2}$ peak position in La_2O_3 varies from 832.5 to 834.9 eV [58]. This great discrepancy in the binding energy values may be explained by the fact that La_2O_3 surface is rapidly

Table 7
XPS characterization of the Bi–La–O oxides obtained by the citrate method (calcination time: 20 h)

Precursor	T (°C)	C1s/ (Bi4f + La3d$_{5/2}$)	Bi4f/ La3d$_{5/2}$	O_{II}/O_I
$Bi_{1/3}La_{2/3}$(citrate)	600	2.39	0.77	1.01
	700	2.45	0.84	1.22
$Bi_{1/2}La_{1/2}$(citrate)	600	2.02	1.49	0.67
	700	1.74	1.55	0.56
$Bi_{2/3}La_{1/3}$(citrate)	600	1.84	2.59	0.60
	700	1.67	2.49	0.49

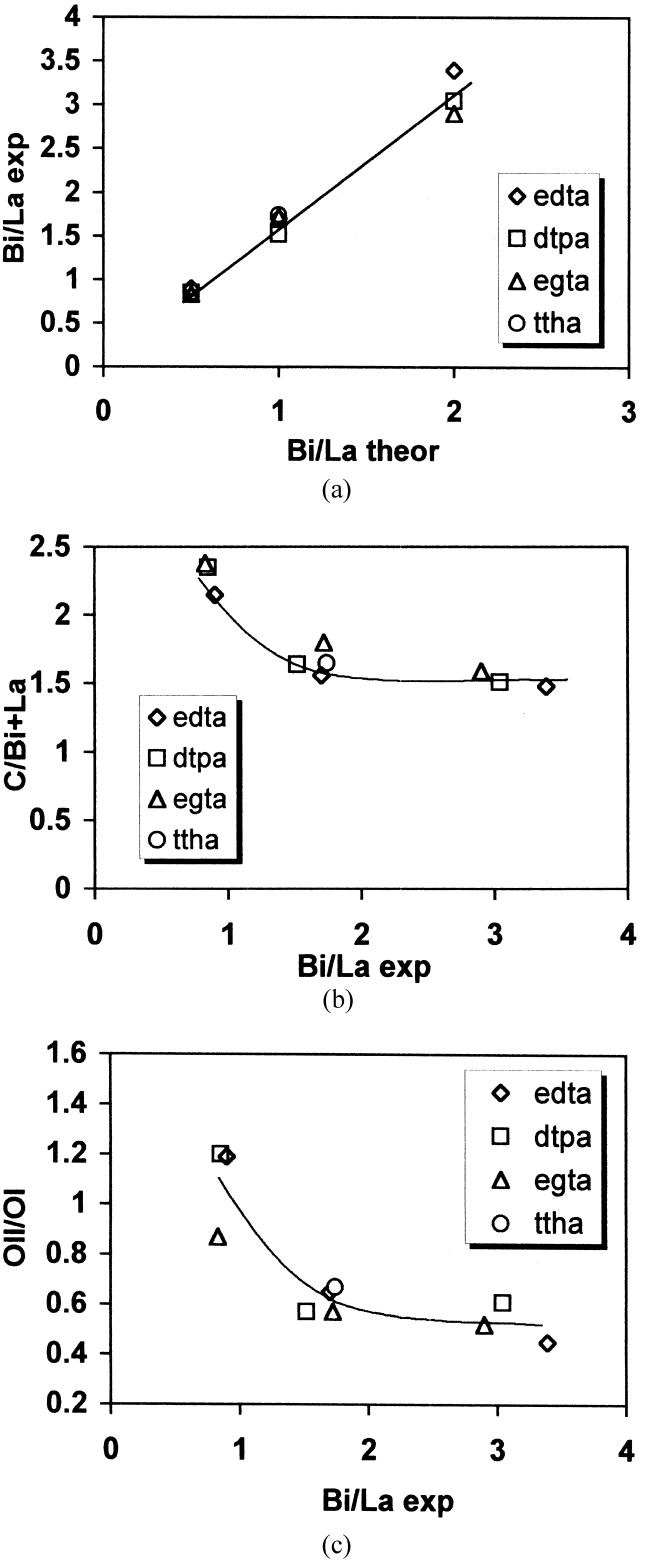

Fig. 6. XPS data of Bi–La–O oxides obtained from polyaminocarboxylate precursors calcined at 600°C for 20 h. (a) Experimental vs. theoretical (Bi 4f/La $3d_{5/2}$) atomic ratios. (b) C 1s/(Bi 4f + La $3d_{5/2}$) atomic ratio vs. (Bi 4f/La $3d_{5/2}$). (c) O(II)/O(I) atomic ratio vs. (Bi 4f/La $3d_{5/2}$).

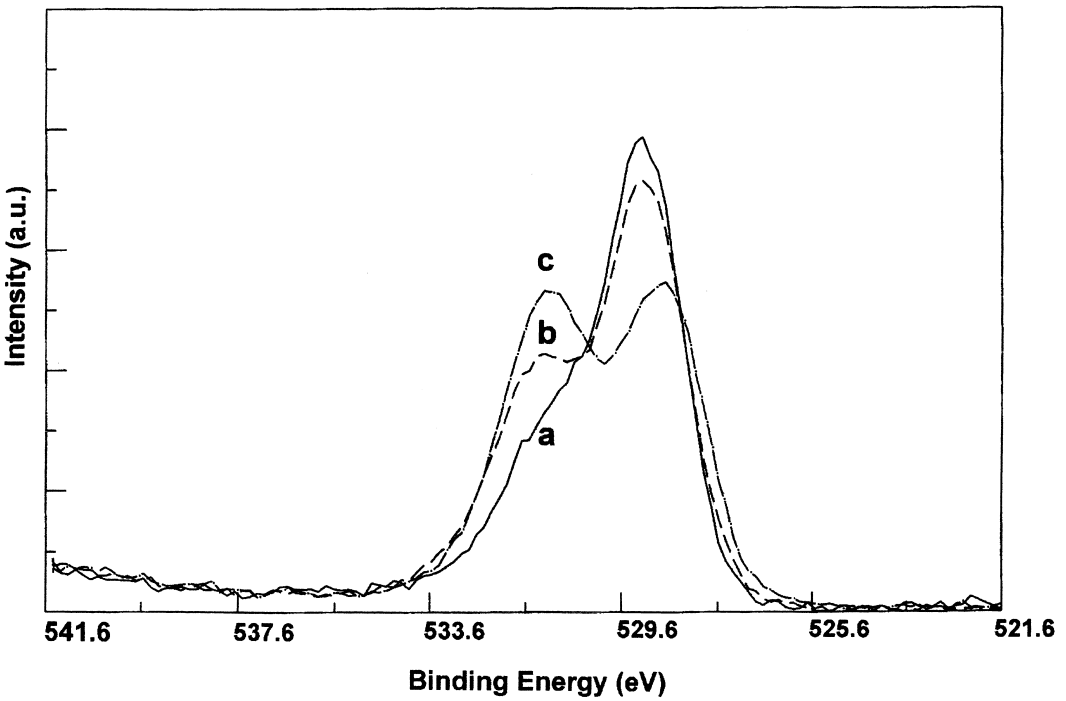

Fig. 7. Oxygen O1s XPS spectra of the Bi–La–O oxides obtained by calcination of $[Bi(edta)]_x[La(edta)]_{1-x}$ precursors ((a) $x=0.67$, (b) $x=0.50$, (c) $x=0.33$) at 600°C for 20 h.

covered by hydroxyl and carbonate species, as mentioned above. An in situ sample treatment is necessary to get a pure clean La_2O_3 surface. It seems that the most realistic value for pure La_2O_3, i.e. the oxide free from hydroxyl or carbonate groups, is 833.4 eV as reported by Haack et al. [59]. The binding energy value of La $3d_{5/2}$ in an old lanthanum carbonate sample has been found at 835.1 eV. This value corresponds exactly to that reported by Galtayries et al. in a La_2O_3 sample aged in air. In accordance with the binding energies values for La $3d_{5/2}$ presented above, the La $3d_{5/2}$ spectrum of our Bi–La–O samples were fitted with two peaks at around 835 and 833 eV, each being accompanied by a satellite. This pattern suggests the existence of two kinds of chemical environments for La^{3+}. The component at higher binding energy can be attributed to hydroxylated/carbonated La^{3+} ions located near the surface and the second one, resembling the pattern of La^{3+} ion in a pure oxide environment may be assigned to La^{3+} ions enclosed in an oxide lattice.

Tables 6 and 7 compare the XPS atomic intensity ratios of the Bi–La–O oxides prepared by the chelate and the citrate methods, respectively. No significant difference can be found in the surface chemical composition between the samples prepared from the PAC precursors and those prepared from citrate precursors. The Bi:La experimental molar ratio is always higher than the theoretical one. As illustrated in Fig. 6a, these values are linearly related with a slope of about 1.6, indicating a surface enrichment in Bi. Similarly, the C/(Bi+La) ratio increases when the overall composition gets richer in La (Fig. 6b) and the O_{II}/O_I ratio follows the same evolution than C/(Bi+La) (Fig. 6c): the proportion of the O_{II} component increases as the samples get richer in La. Fig. 7 illustrates this behaviour in the case of the Bi–Ln edta precursors. Considering the great affinity of lanthanides for carbonate and hydroxyl species, the surface contamination by $-CO_3^{=}$ or –OH groups becomes more important when the Ln content increases.

3.6. Specific surface areas

The results of the surface areas measurements are presented in Tables 8 and 9 for the ceramic and chelate/citrate methods, respectively. The BET specific surface area of the Bi–Ln–O mixed oxides is strongly influenced by the Bi:Ln ratio. The mixed oxides obtained by the ceramic route exhibit surface areas which are in any case lower than 5 m^2/g, the largest values being observed in the Ln-rich region. As far as the chelate method is concerned,

Table 8
BET specific surface areas (m^2/g) of the Bi–Ln (Ln=La, Pr) oxides prepared by the ceramic route

Starting mixture	Bi/Ln			
Calcination conditions	0.33	0.5	1.0	2.0
$Bi_2O_3+La_2O_3$ 800°C 4 h	2.8	–	1.2	–
$Bi_2CO_5+Pr_2(CO_3)_3$ 700°C 48 h	–	4.6	2.7	0.8

Table 9
BET specific surface areas (m^2/g) of the Bi–Ln (Ln=La, Pr) oxides prepared by the chelate and citrate methods

		Bi/Ln=0.5				Bi/Ln=1					Bi/Ln=2			
		edta	dtpa	egta	citrate	edta	dtpa	egta	ttha	citrate	edta	dtpa	egta	citrate
600°C 2 h	La	21.7	22.0	30.0	–	12.0	7.0	11.5	10.6	–	–	4.8	3.0	–
	Pr	–	19.9	31.2	–	–	9.9	13.8	12.9	–	–	8.8	7.7	–
600°C 20 h	La	26.5	23.4	33.6	9.3	22.7	10.1	26.5	12.9	9.2	1.4	3.6	2.9	5.0
	Pr	–	–	–	8.6	–	–	–	–	8.4	–	–	–	3.2
800°C 2 h	La	16.3	15.3	22.0	–	16.0	12.0	9.5	11.9	–	–	0.7	0.2	–
	Pr	–	8.4	9.8	–	–	5.6	7.0	11.2	–	–	2.5	4.0	–

when Bi/Ln=2, the surface area does not exceed 3–4 m^2/g but as the composition gets richer in Ln (La or Pr), the surface increases significantly to reach values of more than 30 m^2/g when Bi/Ln=0.5. The ligand nature seems to have very little influence on the S_{BET} of Bi–Ln–O oxides except for samples prepared from BiLn(ttha) precursors. The surface of these oxides, contrary to the other ones, is apparently very insensitive to calcination conditions. Although sintering is responsible for a decrease in the surface areas of the samples prepared from edta, dtpa or egta as the temperature increases, the influence of calcination temperature on samples prepared from ttha precursors appears to be quite negligible. In most cases, samples prepared from the citrate method exhibit smaller surface areas than oxides prepared from PAC precursors, especially when Bi:Ln=0.5.

4. Conclusions

This work illustrates the potentialities of precursor methods based on the use of polyaminocarboxylate-type ligands as alternative routes to synthesise ternary Bi–Ln–O oxides characterized by various Bi:Ln compositions. This pathway is proven to ensure the generation of pure crystalline phases exhibiting high specific surface areas. In addition, the use of carbon-rich precursors leads to no major carbon contamination of the oxide surfaces. In general, the chelate and citrate methods are shown to provide ternary oxides which cannot be obtained as pure phases by the ceramic method. More particularly, for the equimolar Bi–Ln composition, the decadentate ttha ligand allows one to synthesise heteronuclear Bi–Ln complexes which act as molecular precursors in which the two elements are combined at the molecular level, leading much more readily to the corresponding cubic solid solution.

Acknowledgements

The authors acknowledge financial support from the Belgian National Fund for Scientific Research (FNRS, Brussels). They are grateful to Professor B. Delmon and P. Grange for the access to the XPS equipment.

References

[1] Brazdil JF, Glaeser LC, Grasselli RK. J Catal 1983;81:142.
[2] Mamedov EA. Catal Rev Sci Eng 1994;36:1.
[3] Araujo CA, Cuchiaro JD, McMillan LD, Scott MC, Scott JF. Nature 1995;374:627.
[4] Shuk P, Wiemhöfer H-D, Guth U, Göpel W, Greenblatt M. Solid State Ionics 1996;89:179.
[5] Iwahara H, Esaka T, Sato T, Takahashi T. J Solid State Chem 1981;39:173.
[6] Portefaix N, Conflant P, Boivin JC, Wignacourt JP, Drache M. J Solid State Chem 1997;134:219.
[7] Battle PD, Catlow CRA, Heap JW, Moroney LM. J Solid State Chem 1986;63:8.
[8] Battle PD, Catlow CRA, Moroney LM. J Solid State Chem 1987;67:42.
[9] Abraham F, Boivin JC, Mairesse G, Nowogrocki G. Solid State Ionics 1990;40/41:934.
[10] Maeda H, Tanaka Y, Fukutomi M, Asano T. Jpn J Appl Phys 1988;27:L209.
[11] Nayak R, Suryanarayana A, Rao SB. J Sci Ind Res 1996;55:171.
[12] Endriss H. Bull Bismuth Inst 1995;68:1.
[13] Segal D. In: Chemical synthesis of advanced ceramic materials, London: Cambridge University Press, 1992, pp. 19–20.
[14] Rao CNR, Gopalakrishnan J. Acc Chem Res 1987;20:228.
[15] Marcilly C, Courty P, Delmon B. J Am Ceram Soc 1970;53:56.
[16] Courty P, Ajot H, Marcilly C. Powder Technol 1973;7:21.
[17] Yamamura H, Watanabe A, Shirasaki S, Moriyoshi Y, Tanada M. Ceram Internat 1985;11:17.
[18] Aoki A. Jpn J Appl Phys 1990;29:L270.
[19] Wang NH, Wang CM, Kao HCI, Ling DC, Ku HC, Lii KH. Jpn J Appl Phys 1989;28:L1505.
[20] Chu CT, Dunn B. J Am Ceram Soc 1987;70:C375.
[21] Furcone SL, Chiang YM. Appl Phys Lett 1988;52:2180.
[22] Baythoun MSG, Sale FR. J Mater Sci 1982;17:2757.
[23] Lavados AK, Pomonis PJ. J Chem Soc Faraday Trans 1992;88:2557.
[24] Beltran-Porter D, Martinez-Tamayo E, Ibanez R, Bertran-Porter A, Folgado JV, Escriva E, Munoz V, Segura A, Cantanero A. Mater Res Bull 1988;23:987.
[25] Tanaka N, Wakabayashi H, Mochizuki SI, Ohshio S, Saitoh H. J Mater Res 1998;13:2775.
[26] Fransaer J, Roos JR, Delaey L, Van Der Biest O, Arkens O, Celis JP. J Appl Phys 1989;65:3277.
[27] Fusijawa T, Takagi A, Honjoh T, Okuyama K, Ohshima S, Matsuki K, Muraishi K. Jpn J Appl Phys 1989;28:1358.

[28] Maeda S, Tsurusaki Y, Tachiyama Y, Naka K, Ohki A, Ohgushi T, Takeshita T. J Polymer Sci A: Polymer Chem 1994;32:1729.
[29] van Doorn RHE, Kruidhof H, Nijmeijer A, Winnubst L, Burggraaf AJ. J Mater Chem 1998;8:2109.
[30] Hong L, Guo F, Lin JY. Mater Res Bull 1999;34:1943.
[31] Huang YH, Xu ZG, Yan CH, Wang ZM, Zhu T, Liao CS, Gao S, Xu GX. Solid Stat Commun 2000;114:43.
[32] Sato M, Tanji T, Hara H, Nishide T, Sakashita Y. J Mater Chem 1999;9:1539.
[33] Xu YB, Chen XM, Wu YU. Mater Lett 2000;44:370.
[34] Narendar Y, Messing GL. J Am Ceram Soc 1999;82:1659.
[35] Ma X. Mater Lett 2000;43:170.
[36] Apblett AW, Cubano LA, Georgieva GD, Mague JT. Chem Mater 1996;8:650.
[37] Marrot B, Brouca-Cabarrecq C, Mosset A. J Mater Chem 1996;6:789.
[38] Marrot B, Brouca-Cabarrecq C, Mosset A. J Chem Crystallogr 1998;28:447.
[39] Zhu Y, Yi T, Gao S, Yan C, Cao L. J Mater Sci 1999;34:4969.
[40] Devillers M, Lebrun S, Tirions O, Wullens H. Mat Res Soc Symp Proc 1999;547:203.
[41] Wullens H, Bodart N, Tinant B, Devillers M, in preparation.
[42] Wullens H, Devillers M, Tinant B, Declercq J-P, J Chem Soc Dalton Trans. 1996:2023.
[43] Wullens H, Devillers M, Tinant B, Declercq J-P. Acta Cryst 1998;C54:770.
[44] Summers SP, Abboud KA, Farrah SR, Palenik GJ. Inorg Chem 1994;33:88.
[45] Ruloff R, Prokop P, Sieler J, Hoyer E, Beyer L. Z Naturforsch, 1996;B51:963.
[46] Kornev VI, Trubachev AV. Russ J Inorg Chem 1987;32:1419.
[47] Harwig HA, Gerards AG. J Solid State Chem 1978;26:265.
[48] Medernach JW, Snyder RL. J Am Ceram Soc 1978;61:494.
[49] Harwig HA. Z Anorg Allg Chem 1978;444:151.
[50] McCullough JD. J Am Chem Soc 1950;72:1386.
[51] Shannon RD. Acta Cryst 1976;A32:751.
[52] Bernal S, Botana FJ, Garcia R, Rodriguez-Izquierdo JM. React Solids 1987;4:23.
[53] Bernal S, Botana FJ, Garcia R, Rodriguez-Izquierdo JM. Thermochim Acta 1983;66:139.
[54] Galtayries A, Blanco G, Cifredo GA, Finol D, Gatica JM, Pintado JM, Vidal H, Sproken R, Bernal S. Surf Interface Anal 1999;27:941.
[55] Haack LP, de Vries JE, Otto K, Chattha MS. Appl Catal 1992;82:199.
[56] Shuk P, Wiemhöfer H-D, Göpel W. Z Anorg Allg Chem 1997;623:892.
[57] Burroughs P, Hamnett A, Orchard AF, Thornton G, J Chem Soc Faraday Trans 1976:1686.
[58] Wagner CD, Riggs WM, Davis LE, Moulder JF, Muilenberg GE. In: Handbook of x-ray photoelectron spectroscopy, Eden Prairie, MN: Perkin-Elmer, Physical Electronics Division, 1979, p. 132.
[59] Haack LP, de Vries JE, Otto K, Chattha MS. Appl Catal 1992;82:199.